1-2017

# Lifelong quercetin enrichment and cardioprotection in Mdx/Utrn+/− mice

Christopher Ballmann
*Auburn University*

Thomas S. Denney
*Auburn University*

Ronald J. Beyers
*Auburn University*

Tiffany Quindry
*Auburn University*

Matthew Romero
*Auburn University*

*See next page for additional authors*

# Lifelong quercetin enrichment and cardioprotection in Mdx/Utrn+/− mice


## Abstract

Duchenne Muscular Dystrophy (DMD) is associated with progressive cardiac pathology, however, the SIRT1/PGC1-α activator quercetin may cardioprotect dystrophic hearts. We tested the extent to which long term 0.2% dietary quercetin enrichment attenuates dystrophic cardiopathology in Mdx/Utrn+/- mice. At 2 months, Mdx/Utrn+/- mice were fed quercetin enriched (Mdx/Utrn+/--Q) or control diet (Mdx/Utrn+/-) for 8 months. Control C57BL/10 (C57) animals were fed a control diet for 10 months. Cardiac function was quantified by MRI at 2 and 10 months. Spontaneous physical activity was quantified during the last week of treatment. At 10 months hearts were excised for histological and biochemical analysis. Quercetin feeding improved various physiologic indices of cardiac function in diseased animals. Mdx/Utrn+/--Q also engaged in more high intensity physical activity than controls. Histological analyses of heart tissues revealed higher expression and co-localization of utrophin and α-sarcoglycan. Lower abundance of fibronectin, cardiac damage (Hematoxylin Eosin-Y), and MMP9 were observed in quercetin fed versus control Mdx/Utrn+/- mice. Quercetin evoked higher protein abundance of PGC-1α, cytochrome-c, ETC complexes I-V, citrate synthase, SOD2, and GPX compared to control-fed Mdx/Utrn+/-. Quercetin decreased abundance of inflammatory markers including NFκB, TGF-β1, and F4/80 compared to Mdx/Utrn+/-, however, P-NFκB, P-IKBα, IKBα, CD64 and COX2 were similar between groups. Dietary quercetin enrichment improves cardiac function in aged Mdx/Utrn+/- mice, increases mitochondrial protein content, and dystrophin glycoprotein complex formation. Histological analyses indicate a marked attenuation in pathological cardiac remodeling and indicate that long term quercetin consumption benefits the dystrophic heart.



## Keywords

Polyphenol, Utrophin, Duchenne Muscular Dystrophy

## Disciplines

Agriculture | Animal Experimentation and Research | Animal Sciences | Cardiology | Physiology

## Comments

This is a manuscript of an article published as Ballmann, Christopher, Thomas S. Denney, Ronald J. Beyers, Tiffany Quindry, Matthew Romero, Rajesh Amin, Joshua T. Selsby, and John C. Quindry. "Lifelong quercetin enrichment and cardioprotection in Mdx/Utrn+/− mice." *American Journal of Physiology-Heart and Circulatory Physiology* 312, no. 1 (2017): H128-H140. doi: 10.1152/ajpheart.00552.2016. Posted with permission.



## Authors

Christopher Ballmann, Thomas S. Denney, Ronald J. Beyers, Tiffany Quindry, Matthew Romero, Rajesh Amin, Joshua T. Selsby, and John C. Quindry

Articles in PresS. Am J Physiol Heart Circ Physiol (November 11, 2016). doi:10.1152/ajpheart.00552.2016

# Lifelong quercetin enrichment and cardioprotection in Mdx/Utrn$^{+/-}$mice

Christopher Ballmann[1], Thomas S. Denney[2], Ronald J. Beyers[2], Tiffany Quindry[1], Matthew Romero[1], Rajesh Amin[3], Joshua T. Selsby[4], John C. Quindry [1]

[1]School of Kinesiology, Auburn University, Auburn, AL
[2] MRI Research Center, Auburn University, Auburn, AL
[3] Harrison School of Pharmacy, Auburn University, Auburn, AL
[4]Department of Animal Science, Iowa State University, Ames, IA

**Running Head**: Quercetin Mdx/Utrn$^{+/-}$ mice cardiac pathology

**Address for Correspondence**:
John C. Quindry, PhD, FACSM
Cardioprotection Laboratory
Health and Human Performance
University of Montana
Missoula, MT
Phone (406) 243-4268 Fax (406) 243-6252
Email: john.quindry@mso.umt.edu

**Abstract**

Duchenne Muscular Dystrophy (DMD) is associated with progressive cardiac pathology, however, the SIRT1/PGC1-α activator quercetin may cardioprotect dystrophic hearts. We tested the extent to which long term 0.2% dietary quercetin enrichment attenuates dystrophic cardiopathology in Mdx/Utrn$^{+/-}$ mice. At 2 months, Mdx/Utrn$^{+/-}$ mice were fed quercetin enriched (Mdx/Utrn$^{+/-}$-Q) or control diet (Mdx/Utrn$^{+/-}$) for 8 months. Control C57BL/10 (C57) animals were fed a control diet for 10 months. Cardiac function was quantified by MRI at 2 and 10 months. Spontaneous physical activity was quantified during the last week of treatment. At 10 months hearts were excised for histological and biochemical analysis. Quercetin feeding improved various physiologic indices of cardiac function in diseased animals. Mdx/Utrn$^{+/-}$-Q also engaged in more high intensity physical activity than controls. Histological analyses of heart tissues revealed higher expression and co-localization of utrophin and α-sarcoglycan. Lower abundance of fibronectin, cardiac damage (Hematoxylin Eosin-Y), and MMP9 were observed in quercetin fed versus control Mdx/Utrn$^{+/-}$ mice. Quercetin evoked higher protein abundance of PGC-1α, cytochrome-c, ETC complexes I-V, citrate synthase, SOD2, and GPX compared to control-fed Mdx/Utrn$^{+/-}$. Quercetin decreased abundance of inflammatory markers including NFκB, TGF-β1, and F4/80 compared to Mdx/Utrn$^{+/-}$, however, P-NFκB, P-IKBα, IKBα, CD64 and COX2 were similar between groups. Dietary quercetin enrichment improves cardiac function in aged Mdx/Utrn$^{+/-}$ mice, increases mitochondrial protein content, and dystrophin glycoprotein complex formation. Histological analyses indicate a marked attenuation in pathological cardiac remodeling and indicate that long term quercetin consumption benefits the dystrophic heart.

**Key Words:** Polyphenol, Utrophin, Duchenne Muscular Dystrophy

**Novel findings:** The current investigation provides first time evidence that quercetin provides physiologic cardioprotection against dystrophic pathology and is associated with improved spontaneous physical activity. Secondary findings suggest that quercetin-dependent outcomes are in part due to PGC-1α pathway activation.

## Introduction

Duchenne muscular dystrophy (DMD) is a juvenile musculoskeletal genetic disease of dystrophin deficiency. DMD is caused by a loss of functional dystrophin protein expression due to a nonsense mutation (11) and affects 1 in 3,500 males resulting in a progressive loss of muscle function and premature death (16). Physiologically, DMD is evident by muscle atrophy and weakness with a wide range of heterogeneity. Disease progression is marked by muscle degeneration and inadequate regeneration leading to respiratory and cardiac complications. Failure of the diaphragm and accessory respiratory muscles commonly cause death in many patients resulting in early mortality (15). Due to improvements in care, the average life span of DMD patients has extended to the point that cardiac pathology accounts up to 40% of all deaths (9). As cardiac health deteriorates, cardiac complications manifest as ECG abnormalities, cardiac remodeling, contractile dysfunction, fibrotic tissue deposition, ventricular dilation, and heart failure (17). Accordingly, countermeasures directed against cardiac pathology in the DMD heart are needed.

Several mouse models of DMD exist as first step in the scientific vetting of potential therapeutics for DMD. The dystrophin deficient mdx mouse is currently the most investigated animal model, though disease severity and lifespan in the mdx mouse imperfectly recapitulate the human condition.(14, 40) In contrast, the Mdx/Utrn$^{+/-}$ mouse is a comparatively less studied model of murine DMD that exhibits an exacerbated pathology and reduced life span. The Mdx/Utrn$^{+/-}$ mouse lacks dystrophin and is a heterozygous knockout for utrophin, a dystrophin like protein, which appears to alleviate DMD pathology if upregulated and may partially replace dystrophin deficiency in mdx mice.(41) Furthermore, aged Mdx/Utrn$^{+/-}$ mice exhibit accelerated declines in cardiac health and dystrophic pathology.(50)

Prior work clearly indicates that DMD is a multifaceted disease whereby inflammation, mitochondrial dysfunction, and oxidative stress work in concert to promote cardiac pathology. Accordingly, countermeasures directed against individual disease facets including anti-inflammatory agents, (17) and antioxidant administration(51) attenuate cardiac dysfunction. While ‘cocktail therapies’ are currently used in clinical settings to counter individual aspects of DMD, a single counter measure remains elusive. New findings suggest that a class of flavanones (primarily plant-derived polyphenols) may be effective as a single therapeutic agent in blunting the pathological mechanisms associated with dystrophic cardiopathology.

Polyphenols effectively combat chronic inflammation,(7) cardiac pathology,(20) oxidative stress(48) and induce adaptive gene expression through activation of SIRT1/PGC-1α (24, 27). This latter point is a fundamental mechanism underpinning the benefits of polyphenol use. Early published findings suggest that polyphenols promote induction of adaptive gene transcripts including the SIRT1/PGC-1α axis that promotes upregulation of mitochondrial endogenous antioxidant enzyme and oxidative enzyme content in

addition to utrophin expression.(22) In support, activation of this pathway may attenuate dystrophic pathology in limb muscle as examined with prevention(21, 38) and rescue(22, 23) approaches. Quercetin (3,3',4',5,7-pentahydroxyflaone) ingestion comprises a majority of the total polyphenol ingestion in the normal diet(8) and has gained recent attention as a potential dietary therapeutic. Quercetin is a naturally occurring, flavonol with inherent anti-inflammatory, direct antioxidant effects, and is a potent SIRT1/PGC-1α activator. Recent work from our lab group suggests that six months of dietary quercetin enrichment (0.2%) elevated bioavailable quercetin levels in blood plasma and may serve as a countermeasure against dystrophic muscle pathologies.(24) Moreover, published data from our lab suggests that short term dietary quercetin enrichment promotes mitochondrial biogenesis, endogenous antioxidant protein abundance, and utrophin expression in young mdx mice. Histological analyses further indicated that quercetin consumption, was also associated with lower matrix metalloprotease-9 (MMP-9) expression in young mdx mouse hearts and attenuated cardiac and fibrotic damage in older mdx mice.(3) While early findings are compelling, it is unknown whether long term dietary quercetin enrichment also translates to improved physiologic outcomes. Given these unknowns and the need to explore novel therapeutic approaches in the context of more severe mouse models of DMD, we undertook the current investigation of quercetin efficacy using the Mdx/Utrn$^{+/-}$ mouse model. Experimental considerations included chronic quercetin treatment from 2 months to 10 months of age, incorporation of high resolution MRI cardiac scans, quantification of spontaneous physical activity in senescent animals, and a comprehensive examination of histological and biochemical post mortem outcomes in the resulting cardiac tissues. We hypothesized that long term dietary quercetin enrichment would elicit improved cardiac function, PGC-1α expression and mitochondrial protein content. In addition, we hypothesized that quercetin-fed mice would exhibit less deleterious tissue remodeling and inflammation than control-fed counterparts. Finally, we hypothesized that quercetin-fed mice would exhibit improved physical activity outcomes as compared to control-fed animals.

## Methods

### Study design and animals

The experimental protocol was submitted to and approved by the Auburn University Animal Care and Use Committee and was in accordance with the American Physiological Society. To complete these experiments 2 month old dystrophin deficient mice heterozygous for a utrophin mutation (Mdx/Utrn$^{+/-}$, stock#014563; derived from female homozygous Utrn$^{tm1Ked}$ allele/Dmd$^{mdx}$ allele and male homozygous Utrn$^{tm1Ked}$ allele/hemizygous Dmd$^{mdx}$ allele) and respective C57BL/10SnJ (stock# 000666) mice of the same background strain were purchased from Jackson Laboratories (Jackson Laboratory, Bar Harbor, Maine). During experimentation, all animals were housed on a 12h-12h reverse light-dark cycle. Prior to the initiation of the experiment all mice were maintained on the same AIN93 diet (Bioserve, Flemington, NJ) diet. At 2 months of age, Mdx/Utrn$^{+/-}$ mouse diets consisted of either AIN93 diet (Mdx/Utrn$^{+/-}$, n=8), AIN93 diet or an identical AIN93 diet fortified with 0.2% quercetin-fortified rodent chow (Mdx/Utrn$^{+/-}$-Q, n=8) (Bioserv Inc., Frenchtown, NJ). Control C57/BL10 mice were fed the AIN93 control rodent chow diet (C57, n=8) for the 8 months total experimentation time. All water and food were provided *ad libitum* throughout the experimentation period.

### Functional cardiac assessment (MRI)

To assess cardiac function, mice were scanned at 2 months and 10 months of age using a 7 Telsa (7T) magnetic resonance imaging (MRI) (Siemens, Erlangen, DE). Prior to scanning, mice were anesthetized and maintained with isoflurane during the scan. Cardiac and respiratory rates were monitored with ECG and respiration leads. A rectal temperature probe was used to monitor core temperature which was maintained with a heating pad at 37°C for all cardiac scans. All mice were maintained under anesthesia during the scanning processes via isoflurane. For cardiac scans, all mice were anesthetized with 1% isoflurane, instrumented for ECG and respiration, placed in a custom made quadrature radio frequency coil, and had body temperature maintained at 37±1 C. Prospectively-gated dark-blood cardiac images were acquired as orthoganal2-chamber and 4-chamber long-axes, and transverse mid-ventricular short-axis slices for 3-dim representation of the entire heart. Scan parameters included field of view = 32x32 mm, slice thickness = 1 mm, matrix = 128x128, pixel size = 0.25x0.25 mm, and cine phases = 20.

Cardiac performance was assessed by two trained analysts under blinded conditions. Cinematic audio video interleaves (AVIs) were created to show real-time heart function and aid in determination of end-systole (ES) and end-diastole (ED) points. Cardiac ES and ED volumetric geometries and left-ventricular wall thickness were quantified using Image J software (NIH, Bethesda, MD).(5) For each cardiac variable, correlation analyses were performed to document agreement between blinded analysts (data not shown). Resulting cardiac data from each analyst for each variable were averaged for final data point determination.

MRI T2 mapping of the entire heart was performed as an indirect metric of tissue edema in the 10 month old scans. T2 maps were acquired as a stack of 6-8 short axis slices at TE=10, 20, 40 and 60 ms, TR = 1500 ms, and other parameters same as above for cine scans. Myocardial tissue T2 estimates were calculated from subsequent per-pixel, 4-point, monoexponential curve-fit to the T2 map images.

**Quantification of spontaneous physical activity**

During the final week of treatment, Mdx/Utrn$^{+/-}$ mice from control- and quercetin-fed groups were observed for instances of sitting, grooming, eating/drinking, socializing, standing, walking, wall pacing, running, and jumping. This technique represents an ethogram (repertoire of typical animal activities) using "0-1 recording" method applied across many species.(29) As such, the observance of a mouse performing a particular activity (sitting, grooming, etc.) was recorded as 1. Activity counts were performed on two occasions by two investigators where activity recordings were made in 15 second blocks for a duration of 10 minutes resulting in a total of 40 time periods per observation session. Thus, for the two recording sessions, 20 total minutes of activity were recorded. Activity counts were performed at a common time at the end of the photo light and photo dark housing cycles and resulting scores were averaged. Total activity counts were calculated as n=1/activity, minimum of 40/session. Moreover, to gauge total activity in a single metric, total activity counts for each activity were scaled for the relative metabolic demand and summed into a final value. Specifically, the metric was scaled to the approximate metabolic costs of the various activities (sitting, grooming = 1, eating/drinking, socializing, and standing = 1.5, walking and wall pacing = 2, running = 2.5, jumping =3). As such, higher metric scores are reflective of engagement in more high intensity activities.

**Tissue harvesting and storage**

After the 10 month longitudinal experiment, mice were weighed, and anaesthetized with isoflurane until a surgical plane was established and mice were sacrificed via cardiac excision. Hearts were rinsed in chilled 10mM PBS, weighed, placed in optimum cutting temperature compound (OCT), and frozen in 2-methyl-butane chilled by liquid nitrogen to reduce risk of freeze fracture. After freezing, hearts were stored at -80°C until further analysis.

**Histology and immunofluorescence**

Hearts were cut 10 µm-15 µm thick on a Shandon Cryotome cryostat (-30°C) and set on 1 mm positively charged microscope slides (Fischer Scientific, Pittsburgh, PA, USA). To assess for total cardiac damage, slides were stained by a Hematoxylin and Eosin-Y histological procedure. Accordingly, stained slides were imaged via light microscopy with Nikon software (Melville, NY, USA). 10-15 images were obtained per slide at a magnification of 40x to characterize and confirm consistent representation of each

cardiac cross section. Images were then analyzed using Image J software (NIH, Bethesda, MD, USA). Results of all images were quantified to the total damaged tissue to total healthy tissue ($\mu m^2$). All imaging and analysis was conducted under blinded conditions.

Cardiac expression of utrophin, fibronectin, metalloprotease 9 (MMP9), α-Sarcoglycan, and co-localization of α-Sarcoglycan and utrophin were determined using a histological immunofluorescence detection procedure. Briefly, slides were fixed with a 10% formalin solution, rinsed, and permeabilized with a Triton X-100 in 1% sodium citrate solution. Slides were rinsed in 10mM PBS and blocked with a 3% bovine serum albumin and 20% goat or mouse serum solution. Slides were incubated with primary antibodies for proteins of interest: (Fibronectin, 1:500 dilution; F3648; Sigma-Aldrich), (Utrophin, 1:500 dilution; sc-33700; Santa Cruz Biotechnology), (α-Sarcoglycan, 1:500 dilution; sc-28278; Santa Cruz Biotechnology) MMP9, 1:500 dilution; sc-6840; Santa Cruz Biotechnology). Heart sections were then incubated with corresponding secondary antibodies for Texas Red (TRITC, 1:500; T1-1000; Vector Laboratories Inc.) and/or fluorescein isothiocyanate (FITC) (1:500, sc-2365; Santa Cruz Biotechnology) (1:500, sc-2010; Santa Crus Biotechnology) fluorescent tags. Slides were sealed with 4',6-diamidino-2-phenylindole (DAPI) (Vector Laboratories Inc.) mounting medium and imaged with a fluorescent microscope (Nikon, Melville, NY). Random images (10-15) were obtained as previously discussed with corresponding DAPI, FITC, and TRITC filters. Images were analyzed for mean fluorescent positive pixels were quantified to the examined area ($\mu m^2$) using Nikon Software (Nikon, Melville, NY). All imaging and analyses were conducted under blinded conditions.

**Western blotting**

Heart protein (50μg/sample) was obtained from heart samples and separated using standard SDS-PAGE techniques on 6%-17% polyacrylamide gels through electrophoresis. Proteins were transferred to polyvinylidene difluoride (PVDF) membranes and stained and imaged with Ponceau stain to ensure equal loading. Membranes were exposed to primary antibodies for each protein of interest: (PGC-1α, 1:500 dilution; sc-13067; Santa Cruz Biotechnology), (SOD2, 1:500; sc-30080; Santa Cruz Biotechnology), (Citrate Synthase, 1:500 dilution; sc-390693; Santa Cruz Biotechnology), (Cytochrome-C, 1:500 dilution; sc-7159; Santa Cruz Biotechnology), (Glutathione peroxidase, 1:500; sc-74498; Santa Cruz Biotechnology), (CD64, 1:500 dilution, sc-15364p; Santa Cruz Biotechnology), .), (F4/80, 1:200 dilution; sc-25830; Santa Cruz Biotechnology), (Cyclooxygenase 2, 1:1000; CS-12282; Cell Signaling Technology Inc.), (NFκB, 1:1000 dilution; CS-8242; Cell Signaling Technology Inc.), (Phospho-NFκB, 1:1000 dilution; CS-3033; Cell Signaling Technology Inc.), (IκBα, 1:1000 dilution; CS-4814; Cell Signaling Technology Inc.), (Phospho-IκBα, 1:1000 dilution; CS-2859; Cell Signaling Technology Inc.), (OxPhos Complex Kit, 1:5000 dilution; 457999; Invitrogen), (TGFβ-1, 1:500 dilution; sc-146; Santa Cruz Biotechnology). Membranes were then exposed to corresponding HRP-conjugated secondary antibodies

for chemiluminescence detection: (anti-rabbit IgG HRP linked, 1:1000 dilution; CS-7074; Cell Signaling Technology Inc.), (anti-mouse IgG HRP linked, 1:1000 dilution; CS-7076: Cell Signaling Technology Inc.). Membranes were reprobed and exposed to corresponding normalizing protein primary antibodies: (GAPDH, 1:1000, GenTex) or (α- Tubulin, 1:1000 dilution; DHSB). Corresponding secondary antibodies previously mentioned were used for chemiluminescence detection. Western blots were normalized to corresponding normalizing protein, Ponceau stain, and were analyzed using a UVP LLC digital imaging device (Upland, CA, USA). All experiments and analysis were conducted by a blinded laboratory technician.

**Statistical analyses**

End point measures were analyzed by one way ANOVA. A two-way (strain x treatment) repeated measures (2 month x 10 month) ANOVA was used to test differences in cardiac function using SPSS 20 (IBM, New York City). Tukey post-hoc analyses were performed as indicated. Significance was set at $p \leq 0.05$ *a priori*. Data are presented as mean ± SEM.

## Results

### Animal characteristics

Animal characteristics and measurements are presented in [**Table 1]**. At the end of the treatment periods Mdx/Utrn$^{+/-}$ and Mdx/Utrn$^{+/-}$-Q mice were heavier than C57 controls ($p<0.001$). Heart weights were higher in Mdx/Utrn$^{+/-}$ mice compared to C57 ($p=0.006$). Heart weights normalized to body weight (mg/g) from Mdx/Utrn$^{+/-}$-Q mice were lower than those from C57 mice ($p=0.001$).

### Cardiac function

MRI cardiac function at 2 month and 10 month time points are presented in [**Table 2]**. For C57, untreated Mdx/Utrn$^{+/-}$ and Mdx/Utrn$^{+/-}$-Q mice, representative T1 dark blood cine images of 10 month old heart scans are presented in **Figure 1**. Representative images include mid-ventricular short axis views at end diastolic (ED) and end systolic (ES) time frames. Analysis of 2 month baseline measurements indicate no differences existed between group for 9 of the 11 cardiac performance measures including ejection fraction (EF), stroke volume (SV), cardiac output (CO), end systolic volume (ESV), left ventricular end diastolic dimension (LVEDD), fractional shortening (%FS), systolic wall thickness (SWT) and %SWT. As an exception and in a strain-dependent fashion, end diastolic volume (EDV) at the 2 month analysis was lower in Mdx/Utrn$^{+/-}$ and Mdx/Utrn$^{+/-}$-Q mice while HR was higher. Inexplicably, left ventricular end systolic dimension (LVESD) was lower in Mdx/Utrn$^{+/-}$ versus C57 and Mdx/Utrn$^{+/-}$-Q mice at the 2 month baseline measurement. Similar to the 2 month assessment, HR was higher in 10 month old Mdx/Utrn$^{+/-}$ and Mdx/Utrn$^{+/-}$-Q as compared to C57. No other strain-dependent cardiac differences were observed at the 10 month time point. Moreover, of the cardiac variables determined currently, only ESV and LVESD were indicative of diminished cardiac function in Mdx/Utrn$^{+/-}$ mice. In contrast, and suggestive of improved cardiac function at the 10 month time point, CO, SV, and EF were higher in Mdx/Utrn$^{+/-}$-Q as compared to Mdx/Utrn$^{+/-}$ and C57 mice. Given these findings, it was not surprising that LVESD, %FS, SWT, and %SWT were elevated in 10 month old Mdx/Utrn$^{+/-}$-Q as compared to Mdx/Utrn$^{+/-}$ and C57. T2 mapping images quantified myocardial tissue T2 at the 10 month time point as a metric of tissue edema. Results indicate a significant rise in T2 value from Mdx/Utrn$^{+/-}$ mice, but no differences were observed between C57 and Mdx/Utrn$^{+/-}$-Q **[Figure 2]**.

### Western blotting

Western blotting was performed in hearts harvested at the 10 month sacrifice to assess key protein abundance related to cardiac mitochondrial content, electron transport chain (ETC) complexes, endogenous antioxidant enzymes, inflammatory signaling, and inflammatory mediators, respectively. **Mitochondrial content** - Mean responses for cardiac mitochondrial content (PGC-1α, cytochrome C, and citrate synthase) and representative blots are presented in **[Figure 3A-D]**. A pattern of elevated protein abundance was observed in Mdx/Utrn$^{+/-}$-Q vs Mdx/Utrn$^{+/-}$ for PGC-1α ($p<0.001$), cytochrome C ($p<0.001$), and citrate synthase ($p<0.001$). Interestingly, hearts from Mdx/Utrn$^{+/-}$-Q exhibited higher

PGC-1α (p=0.002) and cytochrome C (p=0.033) as compared to C57. **ETC complex** - Mean responses for cardiac ETC complex content (complexes I-V) and representative blots are presented in **[Figure 4A-F]**. Notably, because complex analysis was performed in a single blot with target proteins between 20Kda-57Kda, sample loading was normalized to Ponceau stain lane density within that range of molecular weights. Importantly, Mdx/Utrn$^{+/-}$-Q exhibited elevated ETC content for complexes I-V, p<0.001 respectively, compared to Mdx/Utrn$^{+/-}$. Moreover, as compared to C57, hearts of 10 month old Mdx/Utrn$^{+/-}$ mice expressed less ETC content for complexes I (p=0.045), III (p=0.007), IV (p=0.012), and V (p=0.003). **Endogenous antioxidant enzymes** - Mean responses for cardiac levels of endogenous antioxidant enzymes (SOD2, and GPX) and representative blots are presented in **[Figure 5A-C]**. These selected endogenous antioxidant enzymes are associated with mitochondria content and cardiac health. SOD2 protein abundance was lower in Mdx/Utrn$^{+/-}$ mice when compared to C57 (p=0.026) and Mdx/Utrn$^{+/-}$-Q (p=0.004). Furthermore, GPX protein content was higher in Mdx/Utrn$^{+/-}$-Q mice when compared to both control C57 (p=0.020) and Mdx/Utrn$^{+/-}$ (p=0.003). **Inflammatory signaling** - Mean responses for cardiac inflammatory signals (NFκB, P-NFκB, IκBα and P-IκBα) and representative blots are presented in **[Figure 6A-E]**. Analyses of blots from 10 month hearts indicate there were no differences between groups for P-NFκB, IκBα and P-IκBα. In contrast, NFκB protein abundance was higher in hearts from Mdx/Utrn$^{+/-}$ mice when compared to Mdx/Utrn$^{+/-}$-Q (p=0.010). **Inflammatory mediators** - Mean responses for cardiac inflammatory mediators (COX-2, TGF-β, F4/80 and CD64) and representative blots are presented in **[Figure 7A-E]**. Analyses of blots from 10 month hearts indicate there were no group differences for COX-2 or CD64. In contrast, Mdx/Utrn$^{+/-}$-Q expressed lower levels of TGF-β (p=0.007) and F4/80 (p=0.049) as compared to hearts from Mdx/Utrn$^{+/-}$ mice.

**Histology**

Histological analyses were performed in hearts harvested at 10 months of age to assess relative protein abundance and localization related to tissue remodeling and DCG assembly. **Tissue remodeling** - Mean histological outcomes for cardiac remodeling (MMP9, fibronectin, and H&E) and representative blots are presented in **[Figure 8A-F]**. Analyses of histological cross sections of hearts from all treatments revealed a common pattern where Mdx/Utrn$^{+/-}$ and Mdx/Utrn$^{+/-}$-Q were higher than C57 for MMP9, fibronectin, and muscle injury. However, and importantly, analyses also revealed profound cardioprotection in quercetin treated animals such that mean values from Mdx/Utrn$^{+/-}$-Q mice were substantially and statistically lower than Mdx/Utrn$^{+/-}$ for MMP9, fibronectin, and muscle injury, respectively. **DGC expression** - Mean histological outcomes for restoration of DGC assembly (utrophin, α-sarcoglycan, and co-localization) and representative images are presented in **[Figure 9A-D]**. Analyses of histological cross sections of hearts from all treatments demonstrated a reduction in DGC assembly in Mdx/Utrn$^{+/-}$ and Mdx/Utrn$^{+/-}$-Q compared to C57 such that utrophin, α-sarcoglycan, and co-localization of the sarcomeric

proteins were lower in diseased animals compared to control. Excitingly, analyses also indicated that mean values from Mdx/Utrn$^{+/-}$-Q mice were higher than Mdx/Utrn$^{+/-}$ for utrophin, α-sarcoglycan, and co-localization, respectively, indicating quercetin-mediated restoration of DGC assembly via increased utrophin abundance and membrane localization.

**Spontaneous physical activity**

Spontaneous physical activity was observed in diseased mice during the final week of treatment. Spontaneous total activity counts are presented in **Table 3**. Analyses indicated similar outcomes for total activity in that Mdx/Utrn$^{+/-}$-Q mice spent less time sitting and more time socializing, standing, walking, wall pacing, running, and jumping. During the observation periods both control- and quercetin-fed Mdx/Utrn$^{+/-}$ mice spent similar times grooming and eating/drinking, the later observation being consistent with body weight similarities. The activity metric results for all nine observed animal activities are presented in **Figure 10**. Findings reveal that Mdx/Utrn$^{+/-}$-Q exhibited significantly more high intensity physical activity as compared to their control-fed counterparts.

## Discussion

In recent years the incidence of cardiac pathology, including heart failure, has become a significant cause of morbidity and mortality in DMD patients.(40) In the absence of an available cure and limited therapeutic approaches, the purpose of this investigation was to pursue a novel and pragmatic therapy to alleviate DMD pathology. The urgency of therapeutic approaches targeting the heart is underscored by an array of promising therapies that effectively attenuate disease progression in skeletal muscle, leading to increased activity and a subsequent cardiac dysfunction. Lifelong 0.2% dietary quercetin enrichment was examined as a countermeasure to cardiac pathology in the Mdx/Utrn$^{+/-}$ mouse; which is noted for its relatively severe disease phenotype.(19) Key dependent cardiac outcomes were examined in concert with a strategic series of post mortem histological and biochemical indices of mitochondrial health, tissue remodeling, and inflammation. Findings reveal for the first time that long term dietary quercetin consumption is a potent intervention against cardiac pathology. In addition to improved histological and biological outcomes in the hearts of quercetin-consuming Mdx/Utrn$^{+/-}$ mice, spontaneous physical activity was greatly improved and suggests improved mobility. As discussed below, the apparent potency of quercetin as an intervention against symptomatic disease progression in dystrophic/utrophic mice may hold important scientific and clinical implications for those with DMD.

### Cardiac function

While young dystrophic mice display relatively healthy cardiac function when compared to age matched controls, dystrophic mice still experience damage due to mechanical overload.(10, 34) Moreover, while well-studied mdx mouse hearts become fibrotic and exhibit early signs of contractile dysfunction by 9 months of age,(40) pathological onset is delayed as compared to humans with DMD. Accordingly, Mdx/Utrn$^{+/-}$ murine model is more severe than mdx and was used in the current study to more closely recapitulate the human disease. Prior investigations report skeletal muscle findings for Mdx/Utrn$^{+/-}$ across the 2 month-to-10 month age range examined currently,(19) in addition to examination of cardiac function in the Mdx/Utrn$^{+/-}$ mouse model.(26, 35) These prior studies employed high strength MRI scans to quantify cardiac function,(26, 35) a methodological approach also used in this investigation. Current findings indicate strain-specific alterations in EDV in the 2 month scan. In this regard, and related to conclusions that can be drawn from anesthetized mice where heart rates are suppressed, it should be noted that HR was higher in both groups of Mdx/Utrn$^{+/-}$ as compared to C57. While this limitation is acknowledged, similar mouse strain-dependent heart rate differences have been observed in comparable aged mice (50). Nonetheless, the existence of heart rate differences between groups could have confounded other cardiac performance variables and possibly interpretation of findings. Accordingly, whenever possible in future investigations it is recommended that anesthesia be titrated to achieve a common heart rate between strains and treatments in an effort to avoid this current study limitation.

Based on the current data and a paucity of published cardiac function data on the Mdx/Utrn$^{+/-}$ mouse, it is difficult to discern whether these pretreatment EDV values represent animal strain-dependent developmental differences and/or early remodeling due to dystrophinopathy. Nonetheless, end of study EDV values were similar between all three groups of mice. Additional research should include additional dosing strategies (e.g., prevention with early treatment versus recovery by dosing later in life after dysfunction has occurred) as a way of better understanding the time course of quercetin efficacy inasmuch as developmental changes in the Mdx/Utrn$^{+/-}$ mouse. Cardiac scans at the end of the 10 month treatment period indicate the existence of a time-dependent pathology was apparent in untreated Mdx/Utrn$^{+/-}$ mice as %SWT was greatly decreased compared to control. Given the anesthetized and unstressed conditions (e.g., independent of β-agonist administration) in which the mice were examined currently, these findings are in general agreement with a paucity of cardiac function studies in Mdx/Utrn$^{+/-}$ mice of a similar age.(50) As a means of potentially discerning subtle differences in treatment- and mouse strain-dependent differences in cardiac function future work with MRI should explore use of cardiac strain analyses.(35)

An important finding in the current investigation is that in 10 month old Mdx/Utrn$^{+/-}$ mice, quercetin-dependent alterations in cardiac function were observed for many of the variables examined, including EF, SV, CO, LVESD, %FS, and SWT. These findings are surprising in that alterations appear to be stimulatory in nature as alterations in cardiac function exceeded that of age-matched C57 mice. The current study design is limited by the fact that a quercetin treated C57 group was not included. Whether C57 treated mice would have experienced similar alterations in cardiac function is uncertain, and as such, this control group should be included in follow-up investigations. While a prior study did not report quercetin-dependent alterations in cardiac function, methodological differences in the mouse strain, quercetin dosing and age limit direct comparison (45). The mechanistic underpinnings of these dramatic findings remain to be determined but may be related to well-described effects of quercetin as a competitive adenosine receptor antagonist (1). If correct, then quercetin appears to have exerted ionotropic effects rather than chronotropic alterations in Mdx/Utrn$^{+/-}$ mice. In support, Bartekova et al. examined quercetin administration as a countermeasure against ischemic injury in doxorubicin treated mice. In quercetin fed mice, they found HR was similar between groups, but significant alterations in indices of left ventricular developed pressure, contractility, and relaxation occurred.(4) The importance of altered cardiac performance in quercetin fed Mdx/Utrn$^{+/-}$ mice are viewed optimistically in light of the parallel observations that histological, biochemical, and animal activity secondary measures support quercetin-dependent improvements into senescence.

Related to cardiac function, both treated and untreated Mdx/Utrn$^{+/-}$ mice were heavier at the end of the investigation as compared to C57 controls. Additional weight gain could be due to fibrosis and edema related to dystrophinopathy. In this regard T2 mapping from 10 month cardiac scans were analyzed as a surrogate marker of myocardial tissue edema, whereby elevated T2 values represent increased tissue water content. Results indicated that T2 values were elevated in Mdx/Utrn$^{+/-}$ mice while Mdx/Utrn$^{+/-}$Q mice were statistically similar to C57. These findings suggest that hearts receiving dietary quercetin were less edemic, a preliminary conclusion that is in agreement with histological findings. Thus, we cannot currently explain the mouse strain-dependent difference in body weight between C57 and both Mdx/Utrn$^{+/-}$ groups.

**Indices of mitochondrial content and oxidative adaptations**

Central to our ongoing research line, dietary quercetin enrichment appears to ameliorate many pathological processes in dystrophic mice via sirtuin1/PGC-1α induction.(3, 22, 24, 38) Flavanones such as quercetin stimulate a variety of physiologic pathways including the SIRT1/PGC-1α axis. Published studies report increased SIRT1/PGC-1α axis gene expression with dietary quercetin feeding,(13, 32) however findings from the current investigation reveal for the first time that long term quercetin enrichment also increases cardiac PGC-1α protein expression. Even more intriguing, quercetin enrichment in Mdx/Utrn$^{+/-}$ mice increased PGC-1α protein expression above that of age matched C57 mice. This latter finding is of particular importance in that heart failure is characterized by decreased PGC-1α expression and decreased mitochondrial function.(49)

Improved indices of mitochondrial content in quercetin fed Mdx/Utrn$^{+/-}$ mice may represent an important link between cardiac function and PGC-1α expression. In the current study a series of mitochondrial related biomarkers were examined in cardiac tissues harvested from 10 month old mice. Findings indicate that quercetin fed mice exhibited higher abundance of citrate synthase, cytochrome-c, and all electron transport complexes 1-V (NADH dehydrogenase, succinate dehydrogenase, cytochrome bc1 complex, cytochrome-C oxidase, and ATP synthase). While not confirmatory, the current data are the first to quantify elevated markers associated with bioenergetic capacity in the dystrophic hearts of Mdx/Utrn$^{+/-}$ mice receiving a quercetin enriched diet. Suggestive of pathology inherent to the DMD animal model, control-fed Mdx/Utrn$^{+/-}$ mice expressed lower abundance of the mitochondrial biomarkers relative to C57 mice. These results emphasize prior observation that dystrophic hearts are susceptible to mitochondrial damage(47) and bolster our earlier observation that cardiac cytochrome-c levels were higher in young mdx mice consuming an identical quercetin diet.(3) While the current finding, in addition to recently published research, suggests that long term quercetin treatment evokes significant metabolic adaptations, (3, 12) the possibility remains that collective findings may reflect a fiber type shift. Mitochondrial outcomes in this investigation are intriguing, albeit indirect measures. As such, additional research is

needed to confirm whether quercetin treatment benefits mitochondrial function. Similar to prior findings in hearts from dystrophin deficient hearts, future investigations should employ direct markers of mitochondrial function within a comprehensive panel of secondary indices of mitochondrial health.(18)

Consistent with increased cardiac mitochondrial content, protein expression of the endogenous antioxidant enzymes SOD2 and GPX were elevated in hearts from Mdx/Utrn$^{+/-}$-Q mice. Although quercetin possess direct antioxidant properties,(6) quercetin also up-regulates endogenous antioxidant enzymes.(3, 48) Since SOD2 is primarily located within mitochondria, increased SOD2 levels bolster our current interpretation that quercetin increased mitochondrial biogenesis in hearts from Mdx/Utrn$^{+/-}$ mice. Furthermore, GPX overexpression attenuates pathological cardiac remodeling and preserves cardiac function in mouse hearts.(30, 39)

The reader is cautioned, however, in the interpretation of these findings (absent of glutathione cycling status) in that alterations in GPX expression may be attributed to redox-induced up-regulation due to elevated $H_2O_2$ production by SOD2. Additional experimentation is needed before firm conclusions about redox status of treated hearts can be conclusively attributed to quercetin consumption. Nonetheless, outcomes from microarray gene profiling experiments of primary cardiomyocytes incubated with quercetin indicate that a host of antioxidant and antioxidant related genes are up-regulated (2). In combination with the anti-inflammatory and anti-proteolytic effects of quercetin on cardiac architecture, a rationale exists that quercetin may also influence phenotypic shifts in fiber type. To our knowledge this latter point is currently untested and should be the focus of additional research efforts.

**DGC protein expression**

Among the most compelling findings of the current investigation is the observation that long term quercetin feeding of Mdx/Utrn$^{+/-}$ mice resulted in improved histological indices of utrophin and α-sarcoglycan. Moreover, protein expression of these fundamental structural proteins appear to be co-localized at the sarcolemma in greater abundance in hearts from quercetin fed mice than in mice maintained on a control diet. These findings are remarkable given the nature of the heterozygous knockout of the utrophin gene in the Mdx/Utrn$^{+/-}$ mouse and support our previous finding of quercetin-related utrophin over expression in mdx mice.(3) Collective findings in the current study are of particular importance in that the real benefit in utrophin up-regulation is dependent upon its role in restoration of the DGC. While current findings are semi-quantitative, these data suggest that quercetin enrichment aids in DCG reassembly in the dystrophic heart.

**Fibrosis and damage**

Histological indices for tissue remodeling reveal strong evidence that long term quercetin feeding of Mdx/Utrn$^{+/-}$ mice lead to profound improvements in age-dependent attenuation in histological remodeling

measures of MMP9, fibronectin, and H&E staining. These findings support our prior work in aged mdx mice exposed to an identical quercetin feeding regimen(3) and emphasize the value of dietary polyphenol use as anti-fibrotic agents.(20, 25) Moreover, current results are in agreement with previous findings that suggest quercetin inhibits MMP9 directly and may also be related to mito- and cyto- protection due to structure–activity analysis demonstrating that flavonoid R3–OH and R4–OH substitutions contribute to MMP9 inhibitory properties.(28, 36) Notably, improvements in quercetin fed Mdx/Utrn$^{+/-}$ mice were not statistically equal to age-matched C57 counterparts. Whether lifetime quercetin feeding (i.e., prior to our 2 month treatment initiation) would have fully attenuated indices of remodeling is uncertain. To better resolve these uncertainties, gross quantification of histological outcomes should be included in future investigations. Nonetheless, complete attenuation pathological remodeling appears unlikely given that remodeling has been observed in younger mdx mice with a less severe dystrophic phenotype.(40) In addition, greater therapeutic effects may be found by combining this quercetin intervention and a complementary intervention with an independent mode of action.

**Indices of inflammatory signaling and mediation**

We observed that quercetin feedings of Mdx/Utrn$^{+/-}$ mice had a modest outcome for attenuation of inflammatory signaling and mediation. This study arm is important given that DMD exhibits multi-faceted physiological maladaptive consequences due to chronic inflammation. Specifically, quercetin enrichment was examined for NFκB pathway activity in Mdx/Utrn$^{+/-}$ hearts. In agreement with a prior finding,(31) total NFκB protein abundance was lower with quercetin feeding, although quercetin enrichment did not alter other examined aspects of the pathway including cardiac levels of IKBα, P-IKBα, and P-NFκB. These largely negative outcomes may be limited by sample collection at a single end point where dynamic signaling changes could not be observed. Accordingly, downstream mediators of NFκB pathway activation (COX-2) and related inflammatory mediators (TGFβ-1, F4/80, and CD64) were also observed. COX 2 protein abundance was ~50% lower in quercetin fed versus control-fed Mdx/Utrn$^{+/-}$ mice, although this finding failed to reach statistical significance. In contrast, TGFβ-1 expression was attenuated with quercetin feeding and supports a previous finding that quercetin blunts fibroblast signaling. (33) Collective findings for TGFβ-1 also bolster the observations of decreased fibronectin expression and cardiac damage in hearts from quercetin fed mdx/Utrn$^{+/-}$ mice. Finally, CD64 and F4/80 were examined as indices of macrophages and immune cell infiltration. Quercetin enrichment did not alter CD64 expression, but was associated with decreased F4/80 protein expression. In concert, these results may suggest that immune cell infiltration in inflammatory signaling decreased, but that any benefits due to dietary quercetin enrichment were modest by comparison to other aspects of this comprehensive investigation.

**Spontaneous activity in Mdx/Utrn$^{+/-}$ mice**

Quercetin treatment elicited significantly more high intensity spontaneous activity in that quercetin-fed mice performed significantly more moderate intensity (socializing and walking) and high intensity (wall pacing, running, and jumping) activity as compared to control-fed Mdx/Utrn$^{+/-}$ mice. Conversely, quercetin-fed mice spent less time sitting. It is important to note that activity scores were averaged across observation periods within the respective dark and light housing cycles. When time-normalized activity counts were scaled for metabolic intensity and incorporated into a single metric, where higher scores reflect more time spent in high intensity activity, it was confirmed that quercetin-fed mice were significantly more active at 10 months of age. This finding of improved physical activity is of vital interest in that 10 month old Mdx/Utrn$^{+/-}$ mice are near the end of their natural lifespan.(46) Anecdotally, activity levels in quercetin fed mice are also higher than 14 month old C57 mice (data not shown currently) and reinforce the aforementioned notion that quercetin may act as an adenosine receptor antagonist. Admittedly, the current investigation is limited by the fact that age matched activity data are not available in C57 mice. Nonetheless, when reflected against the other benefits attributed to quercetin consumption in the current animal-based investigation, improved spontaneous physical activity may hold the most important implications for clinical populations. Furthermore, it is important to recognize broad quercetin-mediated protection in spite of increased activity, which has been linked to negative cardiac outcomes even in cage sedentary animals.(44) Whether the improved cardiac outcomes were due to altered physical activity or the impetus for mice to be more active cannot be determined at this time. In follow-up investigations additional mid-study examination of cardiac function and physical activity are recommended to better delineate the cause and effect of these physiologic outcomes.

**Conclusion**

While multiple published studies reveal flavanone and polyphenol consumption benefits cardiac aging and function,(42, 43) the current investigation is the first to demonstrate that long-term quercetin consumption alleviates cardiac dysfunction in a pathologically severe Mdx/Utrn$^{+/-}$ mouse model of DMD. In addition to the longitudinal approach, this comprehensive data set encompasses physiologic, histological, and biochemical outcomes measured concurrently. Findings reveal that long term dietary quercetin feeding robustly protects against the development of cardiac dysfunction in the Mdx/Utrn$^{+/-}$ mouse. Post mortem cardiac tissue histological and biochemical analyses indicate that quercetin enrichment exerted dramatic improvements in cardiac remodeling and mitochondrial protein markers for oxidative enzymes and endogenous antioxidant enzymes. These noteworthy results bolster our previous investigations using similar methodological approaches in the mdx mouse model of DMD. Collective findings suggest that dietary quercetin consumption exerts pleiotropic benefits in cardiac function that may also extend to improvements in spontaneous physical activity. Of note, these data stand in stark contrast to our recent findings in skeletal muscle where quercetin-mediated protection was transient with

advancing age.(37) We present compelling, albeit indirect, evidence to suggest that increased PGC-1α expression underpins the cardioprotective benefits observed in quercetin fed animals. While no single therapeutic agent exists to attenuate age-dependent cardiac dysfunction in dystrophic hearts, current results suggest that quercetin enrichment may be a novel counter therapy against dystrophic cardiopathology. Further investigation is required to resolve whether dietary quercetin enrichment also holds therapeutic potential for DMD patients.

**Funding**

Work was supported by the Duchenne Alliance and its member foundations (Ryan's Quest, Hope for Gus, Team Joseph, Michael's Cause, Duchenne Now, Zack Heger Foundation, Pietro's Fight, RaceMD, JB's Keys, Romito Foundation, Harrison's Fund, Alex'sWish, and Two Smiles One Hope Foundation) grants 100065 and 100071 to JS and JQ.

**Acknowledgements**

None listed

**Conflicts of interest**

None declared

References


1. **Alexander SP**. Flavonoids as antagonists at A1 adenosine receptors. *Phytother Res* 20: 1009-1012, 2006.
2. **Angeloni C, Leoncini E, Malaguti M, Angelini S, Hrelia P, and Hrelia S**. Role of quercetin in modulating rat cardiomyocyte gene expression profile. *Am J Physiol Heart Circ Physiol* 294: H1233-1243, 2008.
3. **Ballmann C, Hollinger K, Selsby JT, Amin R, and Quindry JC**. Histological and biochemical outcomes of cardiac pathology in mdx mice with dietary quercetin enrichment. *Experimental physiology* 100: 12-22, 2015.
4. **Bartekova M, Simoncikova P, Fogarassyova M, Ivanova M, Okruhlicova L, Tribulova N, Dovinova I, and Barancik M**. Quercetin improves postischemic recovery of heart function in doxorubicin-treated rats and prevents doxorubicin-induced matrix metalloproteinase-2 activation and apoptosis induction. *International journal of molecular sciences* 16: 8168-8185, 2015.
5. **Beyers RJ, Smith RS, Xu Y, Piras BA, Salerno M, Berr SS, Meyer CH, Kramer CM, French BA, and Epstein FH**. T(2) -weighted MRI of post-infarct myocardial edema in mice. *Magn Reson Med* 67: 201-209, 2012.
6. **Boots AW, Haenen GR, and Bast A**. Health effects of quercetin: from antioxidant to nutraceutical. *Eur J Pharmacol* 585: 325-337, 2008.
7. **Boots AW, Wilms LC, Swennen EL, Kleinjans JC, Bast A, and Haenen GR**. In vitro and ex vivo anti-inflammatory activity of quercetin in healthy volunteers. *Nutrition* 24: 703-710, 2008.
8. **Chun OK, Chung SJ, and Song WO**. Estimated dietary flavonoid intake and major food sources of U.S. adults. *J Nutr* 137: 1244-1252, 2007.
9. **Costanza L, and Moggio M**. Muscular dystrophies: histology, immunohistochemistry, molecular genetics and management. *Curr Pharm Des* 16: 978-987, 2010.
10. **Danialou G, Comtois AS, Dudley R, Karpati G, Vincent G, Des Rosiers C, and Petrof BJ**. Dystrophin-deficient cardiomyocytes are abnormally vulnerable to mechanical stress-induced contractile failure and injury. *FASEB J* 15: 1655-1657, 2001.
11. **Darras BT**. Molecular genetics of Duchenne and Becker muscular dystrophy. *J Pediatr* 117: 1-15, 1990.
12. **Davis JM, Murphy EA, Carmichael MD, and Davis B**. Quercetin increases brain and muscle mitochondrial biogenesis and exercise tolerance. *Am J Physiol Regul Integr Comp Physiol* 296: R1071-1077, 2009.
13. **Davis JM, Murphy EA, Carmichael MD, and Davis B**. Quercetin increases brain and muscle mitochondrial biogenesis and exercise tolerance. *Am J Physiol-Reg I* 296: R1071-R1077, 2009.
14. **Dupont-Versteegden EE, and McCarter RJ**. Differential expression of muscular dystrophy in diaphragm versus hindlimb muscles of mdx mice. *Muscle Nerve* 15: 1105-1110, 1992.
15. **Eagle M, Baudouin SV, Chandler C, Giddings DR, Bullock R, and Bushby K**. Survival in Duchenne muscular dystrophy: improvements in life expectancy since 1967 and the impact of home nocturnal ventilation. *Neuromuscul Disord* 12: 926-929, 2002.
16. **Emery AE**. Duchenne muscular dystrophy--Meryon's disease. *Neuromuscul Disord* 3: 263-266, 1993.
17. **Finsterer J, and Cripe L**. Treatment of dystrophin cardiomyopathies. *Nat Rev Cardiol* 11: 168-179, 2014.
18. **Godin R, Daussin F, Matecki S, Li T, Petrof BJ, and Burelle Y**. Peroxisome proliferator-activated receptor gamma coactivator1- gene alpha transfer restores mitochondrial biomass and improves

mitochondrial calcium handling in post-necrotic mdx mouse skeletal muscle. *J Physiol* 590: 5487-5502, 2012.
19. **Gutpell KM, Hrinivich WT, and Hoffman LM**. Skeletal muscle fibrosis in the mdx/utrn+/- mouse validates its suitability as a murine model of Duchenne muscular dystrophy. *PLoS One* 10: e0117306, 2015.
20. **Han JJ, Hao J, Kim CH, Hong JS, Ahn HY, and Lee YS**. Quercetin prevents cardiac hypertrophy induced by pressure overload in rats. *J Vet Med Sci* 71: 737-743, 2009.
21. **Handschin C, Kobayashi YM, Chin S, Seale P, Campbell KP, and Spiegelman BM**. PGC-1alpha regulates the neuromuscular junction program and ameliorates Duchenne muscular dystrophy. *Genes & development* 21: 770-783, 2007.
22. **Hollinger K, Gardan-Salmon D, Santana C, Rice D, Snella E, and Selsby JT**. Rescue of dystrophic skeletal muscle by PGC-1alpha involves restored expression of dystrophin-associated protein complex components and satellite cell signaling. *Am J Physiol Regul Integr Comp Physiol* 305: R13-23, 2013.
23. **Hollinger K, and Selsby JT**. PGC-1alpha gene transfer improves muscle function in dystrophic muscle following prolonged disease progress. *Experimental physiology* 100: 1145-1158, 2015.
24. **Hollinger K, Shanely RA, Quindry JC, and Selsby JT**. Long-term quercetin dietary enrichment decreases muscle injury in mdx mice. *Clin Nutr* 2014.
25. **Hwang JT, Kwon DY, Park OJ, and Kim MS**. Resveratrol protects ROS-induced cell death by activating AMPK in H9c2 cardiac muscle cells. *Genes & nutrition* 2: 323-326, 2008.
26. **Janssen PM, Murray JD, Schill KE, Rastogi N, Schultz EJ, Tran T, Raman SV, and Rafael-Fortney JA**. Prednisolone attenuates improvement of cardiac and skeletal contractile function and histopathology by lisinopril and spironolactone in the mdx mouse model of Duchenne muscular dystrophy. *PLoS One* 9: e88360, 2014.
27. **Lagouge M, Argmann C, Gerhart-Hines Z, Meziane H, Lerin C, Daussin F, Messadeq N, Milne J, Lambert P, Elliott P, Geny B, Laakso M, Puigserver P, and Auwerx J**. Resveratrol improves mitochondrial function and protects against metabolic disease by activating SIRT1 and PGC-1alpha. *Cell* 127: 1109-1122, 2006.
28. **Lee JK, Kwak HJ, Piao MS, Jang JW, Kim SH, and Kim HS**. Quercetin reduces the elevated matrix metalloproteinases-9 level and improves functional outcome after cerebral focal ischemia in rats. *Acta Neurochir (Wien)* 153: 1321-1329; discussion 1329, 2011.
29. **Martin P, and Bateson P**. *Measuring Behavior*. Cambridge, UK: Cambridge University Press, 2007, p. 171.
30. **Matsushima S, Kinugawa S, Ide T, Matsusaka H, Inoue N, Ohta Y, Yokota T, Sunagawa K, and Tsutsui H**. Overexpression of glutathione peroxidase attenuates myocardial remodeling and preserves diastolic function in diabetic heart. *Am J Physiol Heart Circ Physiol* 291: H2237-2245, 2006.
31. **Min YD, Choi CH, Bark H, Son HY, Park HH, Lee S, Park JW, Park EK, Shin HI, and Kim SH**. Quercetin inhibits expression of inflammatory cytokines through attenuation of NF-kappaB and p38 MAPK in HMC-1 human mast cell line. *Inflamm Res* 56: 210-215, 2007.
32. **Nieman DC, Williams AS, Shanely RA, Jin F, McAnulty SR, Triplett NT, Austin MD, and Henson DA**. Quercetin's influence on exercise performance and muscle mitochondrial biogenesis. *Med Sci Sports Exerc* 42: 338-345, 2010.
33. **Phan TT, Lim IJ, Chan SY, Tan EK, Lee ST, and Longaker MT**. Suppression of transforming growth factor beta/smad signaling in keloid-derived fibroblasts by quercetin: implications for the treatment of excessive scars. *J Trauma* 57: 1032-1037, 2004.
34. **Quinlan JG, Hahn HS, Wong BL, Lorenz JN, Wenisch AS, and Levin LS**. Evolution of the mdx mouse cardiomyopathy: physiological and morphological findings. *Neuromuscul Disord* 14: 491-496, 2004.

35. **Rafael-Fortney JA, Chimanji NS, Schill KE, Martin CD, Murray JD, Ganguly R, Stangland JE, Tran T, Xu Y, Canan BD, Mays TA, Delfin DA, Janssen PM, and Raman SV**. Early treatment with lisinopril and spironolactone preserves cardiac and skeletal muscle in Duchenne muscular dystrophy mice. *Circulation* 124: 582-588, 2011.
36. **Saragusti AC, Ortega MG, Cabrera JL, Estrin DA, Marti MA, and Chiabrando GA**. Inhibitory effect of quercetin on matrix metalloproteinase 9 activity molecular mechanism and structure-activity relationship of the flavonoid-enzyme interaction. *European journal of pharmacology* 644: 138-145, 2010.
37. **Selsby JT, Ballmann CG, Spaulding HR, Ross JW, and Quindry JC**. Oral quercetin administration transiently protects respiratory function in dystrophin deficient mice. *J Physiol* 2016.
38. **Selsby JT, Morine KJ, Pendrak K, Barton ER, and Sweeney HL**. Rescue of dystrophic skeletal muscle by PGC-1alpha involves a fast to slow fiber type shift in the mdx mouse. *PLoS One* 7: e30063, 2012.
39. **Shiomi T, Tsutsui H, Matsusaka H, Murakami K, Hayashidani S, Ikeuchi M, Wen J, Kubota T, Utsumi H, and Takeshita A**. Overexpression of glutathione peroxidase prevents left ventricular remodeling and failure after myocardial infarction in mice. *Circulation* 109: 544-549, 2004.
40. **Shirokova N, and Niggli E**. Cardiac phenotype of Duchenne Muscular Dystrophy: insights from cellular studies. *J Mol Cell Cardiol* 58: 217-224, 2013.
41. **Squire S, Raymackers JM, Vandebrouck C, Potter A, Tinsley J, Fisher R, Gillis JM, and Davies KE**. Prevention of pathology in mdx mice by expression of utrophin: analysis using an inducible transgenic expression system. *Hum Mol Genet* 11: 3333-3344, 2002.
42. **Sulaiman M, Matta MJ, Sunderesan NR, Gupta MP, Periasamy M, and Gupta M**. Resveratrol, an activator of SIRT1, upregulates sarcoplasmic calcium ATPase and improves cardiac function in diabetic cardiomyopathy. *Am J Physiol Heart Circ Physiol* 298: H833-843, 2010.
43. **Thandapilly SJ, Wojciechowski P, Behbahani J, Louis XL, Yu L, Juric D, Kopilas MA, Anderson HD, and Netticadan T**. Resveratrol prevents the development of pathological cardiac hypertrophy and contractile dysfunction in the SHR without lowering blood pressure. *Am J Hypertens* 23: 192-196, 2010.
44. **Townsend D, Yasuda S, Chamberlain J, and Metzger JM**. Cardiac consequences to skeletal muscle-centric therapeutics for Duchenne muscular dystrophy. *Trends in cardiovascular medicine* 19: 50-55, 2009.
45. **Ulasova E, Perez J, Hill BG, Bradley WE, Garber DW, Landar A, Barnes S, Prasain J, Parks DA, Dell'Italia LJ, and Darley-Usmar VM**. Quercetin prevents left ventricular hypertrophy in the Apo E knockout mouse. *Redox Biol* 1: 381-386, 2013.
46. **van Putten M, Hulsker M, Young C, Nadarajah VD, Heemskerk H, van der Weerd L, t Hoen PA, van Ommen GJ, and Aartsma-Rus AM**. Low dystrophin levels increase survival and improve muscle pathology and function in dystrophin/utrophin double-knockout mice. *FASEB J* 27: 2484-2495, 2013.
47. **Vandebrouck A, Ducret T, Basset O, Sebille S, Raymond G, Ruegg U, Gailly P, Cognard C, and Constantin B**. Regulation of store-operated calcium entries and mitochondrial uptake by minidystrophin expression in cultured myotubes. *FASEB J* 20: 136-138, 2006.
48. **Vasquez-Garzon VR, Arellanes-Robledo J, Garcia-Roman R, Aparicio-Rautista DI, and Villa-Trevino S**. Inhibition of reactive oxygen species and pre-neoplastic lesions by quercetin through an antioxidant defense mechanism. *Free Radic Res* 43: 128-137, 2009.
49. **Ventura-Clapier R, Garnier A, and Veksler V**. Transcriptional control of mitochondrial biogenesis: the central role of PGC-1alpha. *Cardiovasc Res* 79: 208-217, 2008.
50. **Verhaart IE, van Duijn RJ, den Adel B, Roest AA, Verschuuren JJ, Aartsma-Rus A, and van der Weerd L**. Assessment of cardiac function in three mouse dystrophinopathies by magnetic resonance imaging. *Neuromuscul Disord* 22: 418-426, 2012.

688 51. **Williams IA, and Allen DG**. The role of reactive oxygen species in the hearts of dystrophin-
689 deficient mdx mice. *Am J Physiol Heart Circ Physiol* 293: H1969-1977, 2007.

690

691

**Figure 1. Representative images of MRI heart scans in 10 month old mice.** Representative T1 dark-blood cine images of MRI heart scans in 10 month old mice. Images include mid-ventricular short-axis views at end-diastole and end-systole time frames from C57 (C57BL/10SnJ), Mdx/Utrn$^{+/-}$, and Mdx/Utrn$^{+/-}$-Q mice. N=6-8/group.

**Figure 2. T2 weighted images from cardiac MRI scans in 10 month old C57 and Mdx/Utrn$^{+/-}$ mice.** T2 weighted images from cardiac MRI scans in 10 month old mice were quantified as an indirect measure of tissue edema. Data are means ± SEM. ***** denotes significantly different from C57 (C57BL/10SnJ), # denotes significantly different from Mdx/Utrn$^{+/-}$.

**Figure 3. Protein abundance of markers of mitochondrial content from 10 month heart tissue.** A) PGC-1α abundance, B) Cytochrome-C abundance, C) Citrate Synthase abundance, and D) representative blots for target proteins and normalization proteins. Samples were derived from ventricular tissue of C57 (C57BL/10SnJ), Mdx/Utrn$^{+/-}$, and Mdx/Utrn$^{+/-}$-Q mice. N=6-8/group. Data are means ± SEM. ***** denotes significantly different from C57, # denotes significantly different from Mdx/Utrn$^{+/-}$.

**Figure 4. Protein abundance of electron transport complexes from 10 month heart tissue.** A) Complex 1 abundance, B) Complex 2 abundance, C) Complex 3 abundance, D) Complex 4 abundance, E) Complex 5 abundance, and F) representative blots and ponceau stained normalization blot. Samples were derived from ventricular tissue of C57 (C57BL/10SnJ), Mdx/Utrn$^{+/-}$, and Mdx/Utrn$^{+/-}$-Q mice. N=6-8/group. Data are means ± SEM. # denotes significantly different from Mdx/Utrn$^{+/-}$.

**Figure 5. Protein abundance of endogenous antioxidant enzymes from 10 month heart tissue.** A) SOD2 abundance, B) GPX abundance, and C) representative blots and normalization proteins. Samples were derived from ventricular tissue of C57 (C57BL/10SnJ), Mdx/Utrn$^{+/-}$, and Mdx/Utrn$^{+/-}$-Q mice. N=6-8/group. Data are means ± SEM. ***** denotes significantly different from C57, # denotes significantly different from Mdx/Utrn$^{+/-}$.

**Figure 6. Protein abundance of inflammatory signaling markers from 10 month heart tissue.** A) NFκB abundance, B) P-NFκB abundance, C) IκBα abundance, D) P-IκBα abundance, and E) representative and normalization protein blots. Samples were derived from ventricular tissue of C57 (C57BL/10SnJ), Mdx/Utrn$^{+/-}$, and Mdx/Utrn$^{+/-}$-Q mice. N=6-8/group. Data are means ± SEM. ***** denotes significantly different from C57.

**Figure 7. Protein abundance of inflammatory mediators from 10 month heart tissue.** A) COX-2, B) TGF-β1, C) F4/80, D) CD64 abundance, and E) representative and normalization protein blots. Samples were derived from ventricular tissue of C57 (C57BL/10SnJ), Mdx/Utrn$^{+/-}$, and Mdx/Utrn$^{+/-}$-Q mice. N=6-8/group. Data are means ± SEM. ***** denotes significantly different from C57, **#** denotes significantly different from Mdx/Utrn$^{+/-}$.

**Figure 8. Histological indices of remodeling from 10 month heart tissue.** A) MMP9 mean densities, B) representative fluorescent micrographs for MMP9, C) fibronectin mean densities, D) representative fluorescent micrographs for fibronectin, E) hematoxylin and eosin mean densities, and F) representative fluorescent micrographs for hematoxylin and eosin. Samples were derived from ventricular cross sections of C57 (C57BL/10SnJ), Mdx/Utrn$^{+/-}$, and Mdx/Utrn$^{+/-}$-Q mice. N=6-8/group. Data are means ± SEM. ***** denotes significantly different from C57, **#** denotes significantly different from Mdx/Utrn$^{+/-}$.

**Figure 9. Histological indices of utrophin expression from 10 month heart tissue.** A) utrophin mean densities, B) α-sarcoglycan mean densities, C) utrophin-α-sarcoglycan colocalization mean densities, D) representative fluorescent micrographs for DAPI (nuclei), FITC (utrophin), TRITC (α-sarcoglycan), FITC+TRITC, and computer merged images of DAPI+FITC+TRITC images. Samples were derived from ventricular cross sections of C57 (C57BL/10SnJ), Mdx/Utrn$^{+/-}$, and Mdx/Utrn$^{+/-}$-Q mice. N=6-8/group. Data are means ± SEM. ***** denotes significantly different from C57, **#** denotes significantly different from Mdx/Utrn$^{+/-}$.

**Figure 10. Spontaneous activity metric scores in Mdx/Utrn$^{+/-}$ mice.**
Composite spontaneous activity score scaled for relative metabolic intensity of sitting, grooming, eating/drinking, socializing, standing, walking, wall pacing, running, and jumping. Scores represent average activity counts during light and dark housing cycles in Mdx/Utrn$^{+/-}$ and Mdx/Utrn$^{+/-}$-Q mice. N=6-8/group. Data are means ± SEM. **#** denotes significantly different from Mdx/Utrn$^{+/-}$.

**Table 1. Animal Characteristics at 10 months**

| Strain | Body Weight (g) | Absolute Heart Weight (mg) | Relative Heart Weight (mg/g) |
|---|---|---|---|
| **C57** | 30.8 ± 2.50 | 162 ± 11.45 | 5.2 ± 0.33 |
| **Mdx/Utrn$^{+/-}$** | 41.2 ± 2.73 * | 194 ± 15.31* | 4.8 ± 0.38 |
| **Mdx/Utrn$^{+/-}$-Q** | 42.0 ± 2.34 * | 183 ± 13.6 | 4.4 ± 0.42 * |

N=6-8/group. Data are means ± SEM; * denotes significantly different from C57.

**Table 2**. **Cardiac Function**

| Time | Strain | HR (bpm) | LV EF (%) | SV (µL) | CO (µL/min) | EDV (µL) | ESV (µL) | LVEDD (mm) | LVESD (mm) | LV FS (%) | SWT (mm) | SWT (%) |
|---|---|---|---|---|---|---|---|---|---|---|---|---|
| **2 month** | **C57** | 333.5±7.4 | 52.3±2.8 | 40.7±2.3 | 14241±422 | 78.5±0.9 | 38.3±2.3 | 3.74±0.04 | 2.25±0.11 | 40.0±2.7 | 0.39±0.05 | 30.3±2.3 |
| | **Mdx/Utrn$^{+/-}$** | 376.5±6.4* | 54.5±2.0 | 33.1±2.1 | 12443±844 | 59.3±3.5* | 27.5±1.8 | 3.07±0.13 | 1.71±0.09* | 44.1±2.2 | 0.36±0.05 | 24.0±2.8 |
| | **Mdx/Utrn$^{+/-}$-Q** | 387.1±8.5* | 51.8±3.5 | 35.4±1.8 | 13105±558 | 66.8±4.3* | 33.2±3.9 | 3.26±0.17 | 1.98±0.18 | 39.7±3.6 | 0.35±0.05 | 26.1±2.8 |
| **10 month** | **C57** | 314.2±14.7 | 53.9±3.2 | 45.0±2.4 | 14308±1320 | 84.5±3.4 | 39.5±4.4 | 3.91±0.08 | 2.21±0.16 | 43.8±3.0 | 0.57±0.04 | 36.2±2.4 |
| | **Mdx/Utrn$^{+/-}$** | 360.0±3.3* | 51.0±1.8 | 41.4±2.4ǂ | 14910±555 | 84.5±3.8ǂ | 41.5±3.0ǂ | 3.71±0.09 | 2.26±0.13ǂ | 39.3±2.5 | 0.47±0.04 | 28.3±2.6* |
| | **Mdx/Utrn$^{+/-}$-Q** | 370.1±7.2* | 62.5±4.4#ǂ | 52.7±2.0*#ǂ | 19852±2818*#ǂ | 81.6±3.3ǂ | 29.4±3.8 | 3.55±0.18 | 1.51±0.11*# | 52.8±5.3*#ǂ | 0.70±0.06#ǂ | 37.4±2.5#ǂ |

Heart rate (HR), left ventricular ejection fraction (LV EF), stroke volume (SV), cardiac output (CO), end diastolic volume (EDV), end systolic volume (ESV), left ventricular end diastolic dimension (LVEDD), left ventricular end systolic dimension (LVESD), left ventricular fractional shortening (LV FS), systolic wall thickness (SWT); N=6-8/group. Data are means ± SEM; ***** denotes significantly different from age matched C57; **#** denotes significantly different from age matched Mdx/Utrn$^{+/-}$; **ǂ** denotes significantly different from 2 month baseline value.

**Table 3**. **Spontaneous animal activity counts in 10 month old Mdx/Utrn$^{+/-}$ mice.**

| | | Activity counts | | | | | | | | |
|---|---|---|---|---|---|---|---|---|---|---|
| **Time** | **Treatment** | **Sitting/ Still** | **Grooming** | **Eat/Drink** | **Socialize** | **Stand** | **Walk** | **Wall Pace** | **Run** | **Jump** |
| **10 month** | **Mdx/Utrn$^{+/-}$** | 29.5 ± 2.5 | 12.8 ± 3.2 | 3.2 ± 1.3 | 1.5 ± 0.8 | 4.6 ± 1.3 | 10.3 ± 2.7 | 1.3 ± 0.5 | 0.6 ± 0.6 | 0.0 ± 0.0 |
| | **Mdx/Utrn$^{+/-}$-Q** | 9.3 ± 0.8# | 10.4 ± 0.8 | 4.1 ± 0.8 | 8.0 ± 0.5# | 16.8 ± 2.3# | 24.4 ± 1.6# | 28.9 ± 2.3# | 6.8 ± 2.5# | 9.0 ± 2.0# |

N=6-8/group. Data are means ± SEM; * denotes significantly different from age matched C57; ǂ denotes significantly different from 2 month baseline value.

775

776
777

**Figure 1**

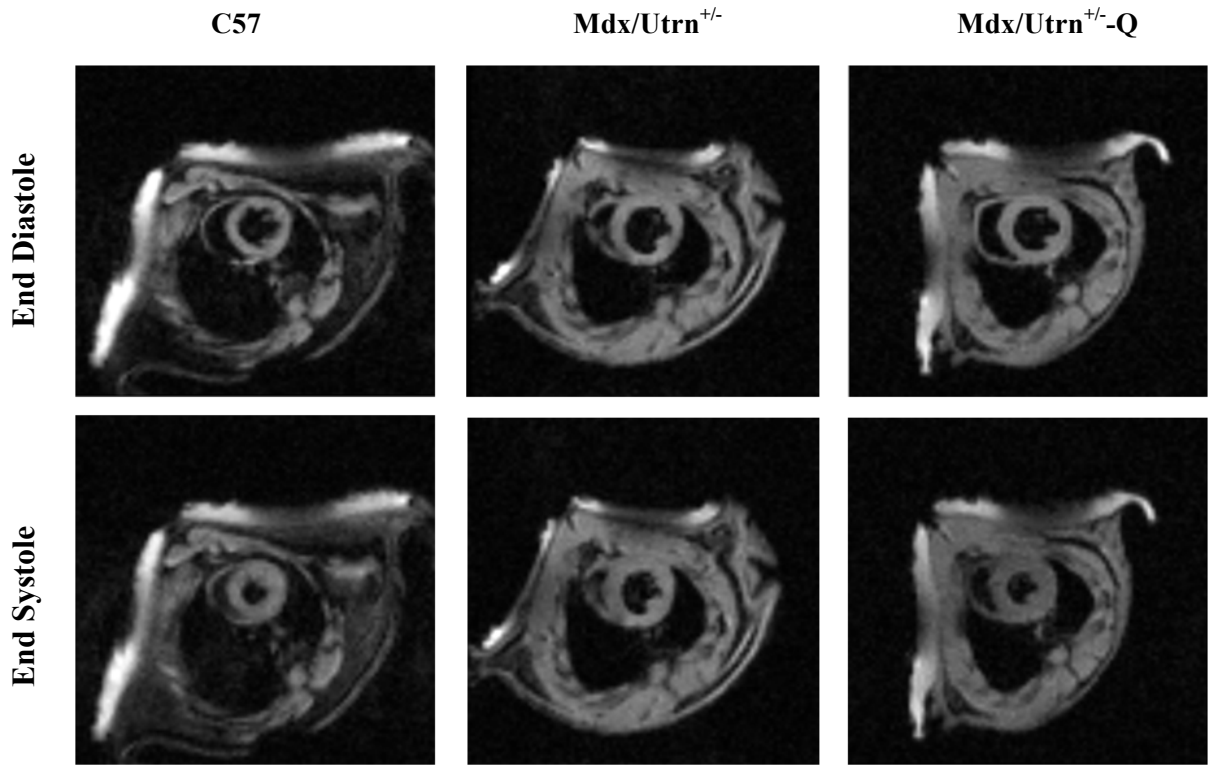

**Figure 2**

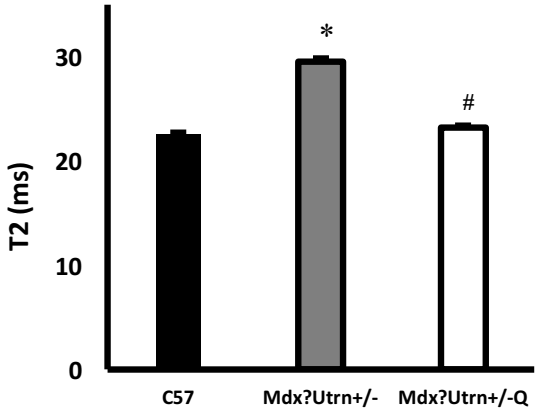

**Figure 3**

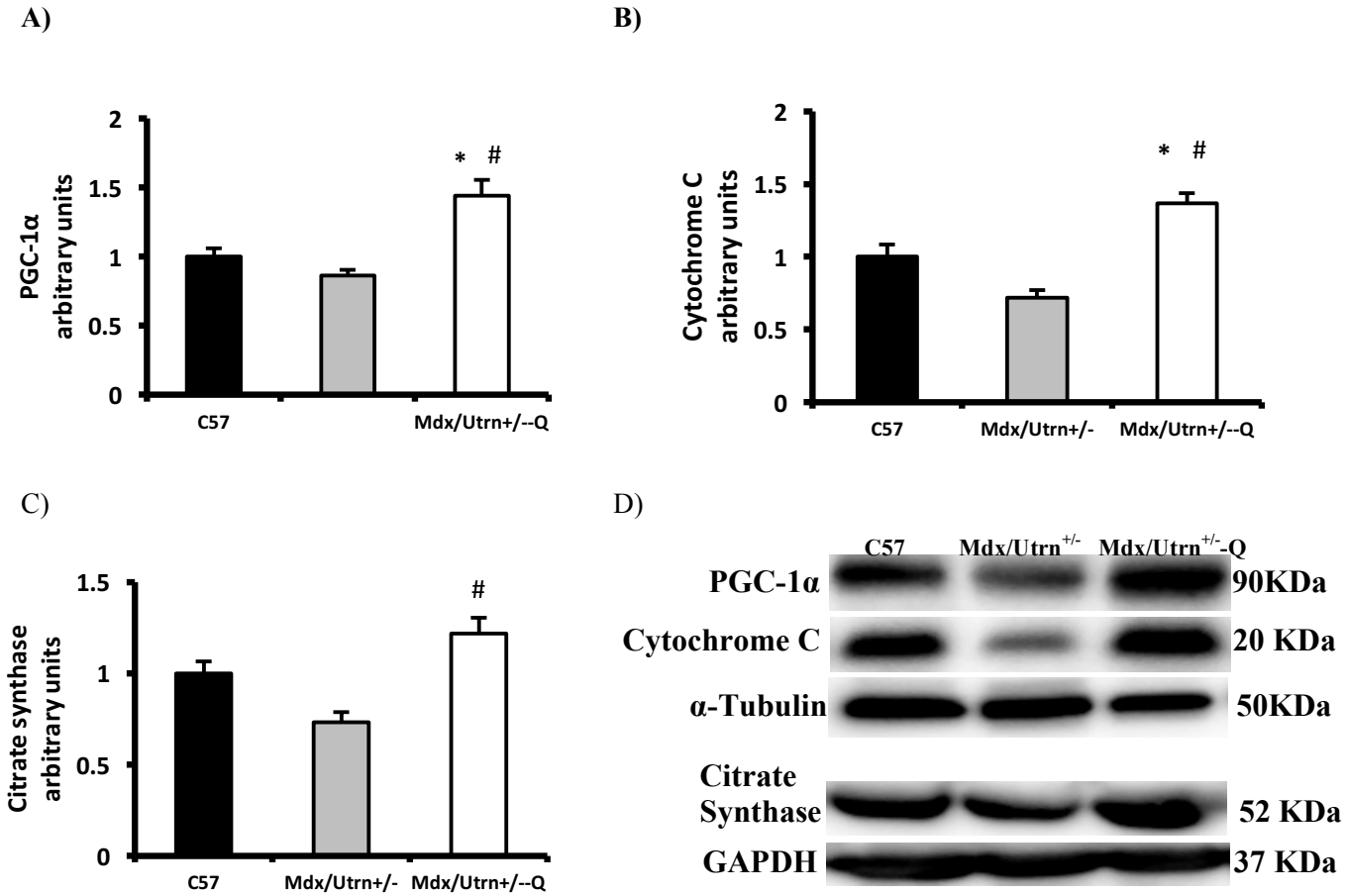
A)
PGC-1α arbitrary units
2
1.5
1
0.5
0
* #
C57
Mdx/Utrn+/--Q
B)
Cytochrome C arbitrary units
2
1.5
1
0.5
0
* #
C57
Mdx/Utrn+/-
Mdx/Utrn+/--Q
C)
Citrate synthase arbitrary units
1.5
1
0.5
0
#
C57
Mdx/Utrn+/-
Mdx/Utrn+/--Q
D)
C57
Mdx/Utrn+/-
Mdx/Utrn+/--Q
PGC-1α
90KDa
Cytochrome C
20 KDa
α-Tubulin
50KDa
Citrate Synthase
52 KDa
GAPDH
37 KDa

**Figure 4**

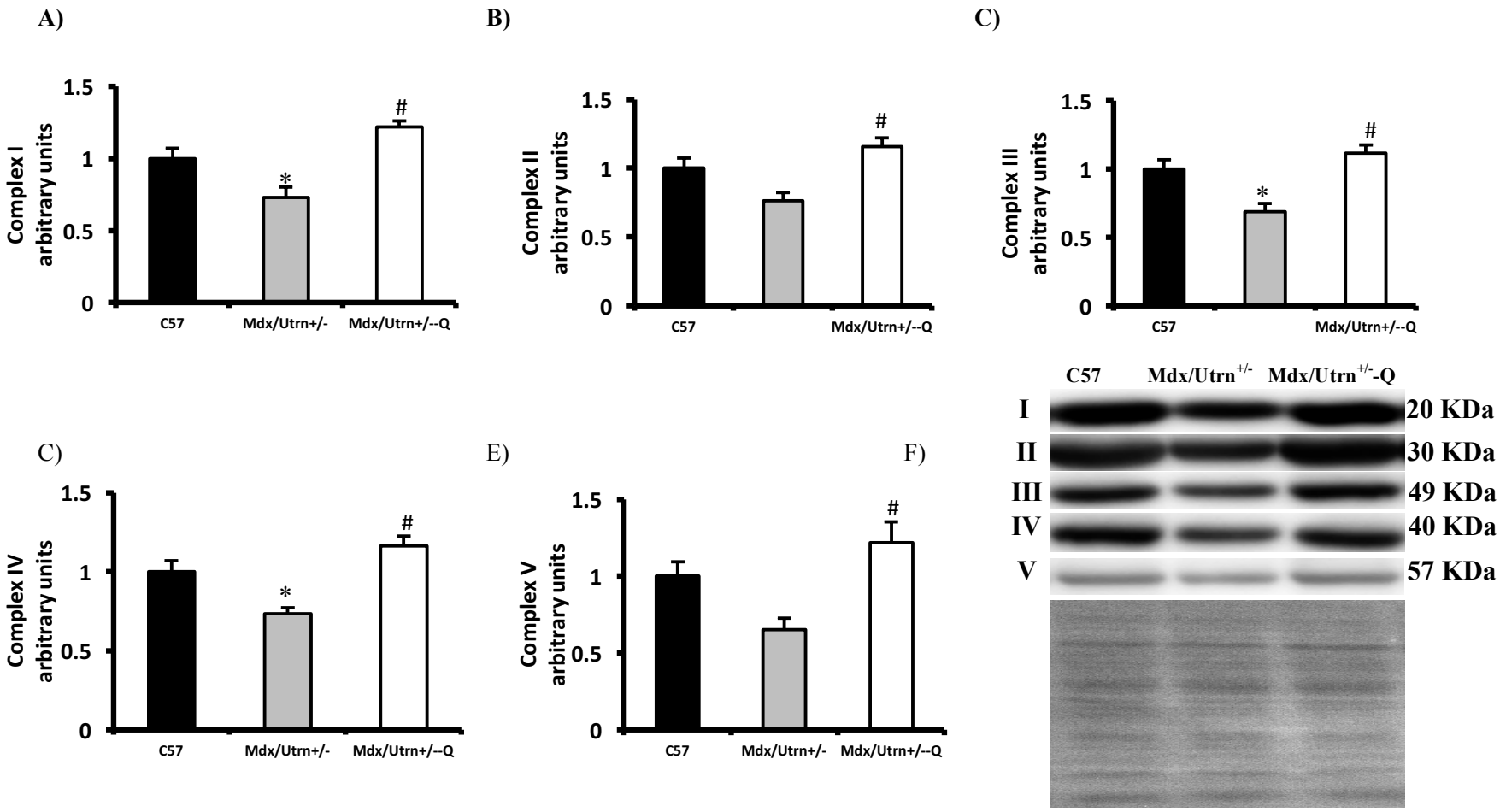
A)
B)
C)
Complex I arbitrary units
Complex II arbitrary units
Complex III arbitrary units
1.5
1
0.5
0
*
#
C57
Mdx/Utrn+/-
Mdx/Utrn+/--Q
C)
E)
F)
Complex IV arbitrary units
Complex V arbitrary units
C57
Mdx/Utrn+/-
Mdx/Utrn+/--Q
C57
Mdx/Utrn+/-
Mdx/Utrn+/-Q
I
II
III
IV
V
20 KDa
30 KDa
49 KDa
40 KDa
57 KDa

**Figure 5**

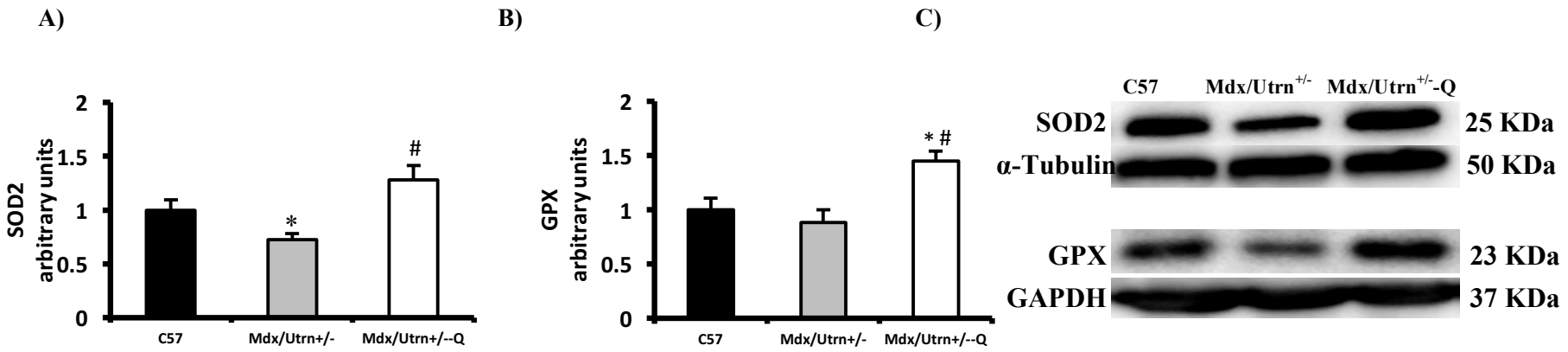
A)
B)
C)
SOD2 arbitrary units
2
1.5
1
0.5
0
*
#
C57
Mdx/Utrn+/-
Mdx/Utrn+/--Q
GPX arbitrary units
* #
C57
Mdx/Utrn+/-
Mdx/Utrn+/--Q
C57
Mdx/Utrn+/-
Mdx/Utrn+/--Q
SOD2
25 KDa
α-Tubulin
50 KDa
GPX
23 KDa
GAPDH
37 KDa

**Figure 6**

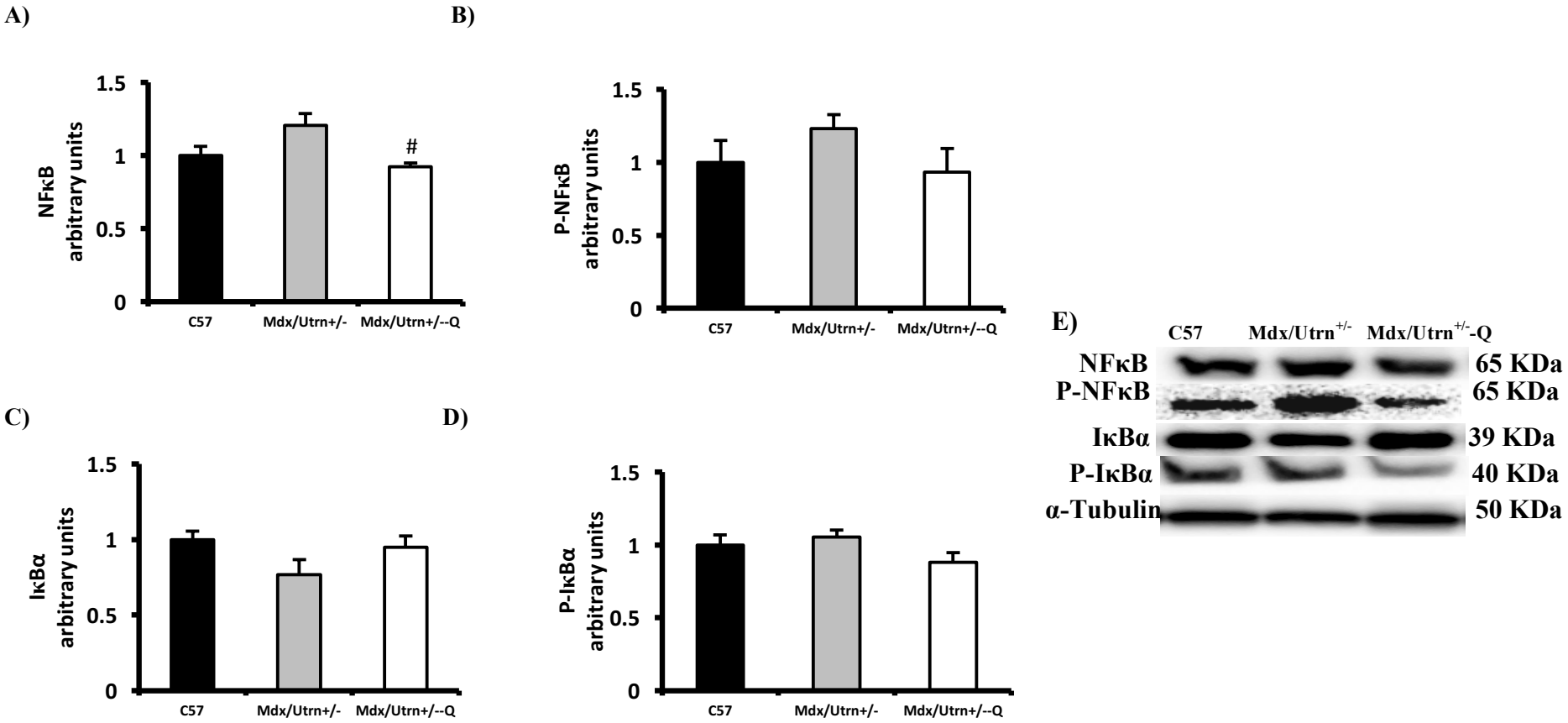
A)
B)
C)
D)
E)
NFκB arbitrary units
P-NFκB arbitrary units
IκBα arbitrary units
P-IκBα arbitrary units
1.5
1
0.5
0
#
C57
Mdx/Utrn+/-
Mdx/Utrn+/--Q
C57
Mdx/Utrn+/-
Mdx/Utrn+/-Q
NFκB
P-NFκB
IκBα
P-IκBα
α-Tubulin
65 KDa
65 KDa
39 KDa
40 KDa
50 KDa

**Figure 7**

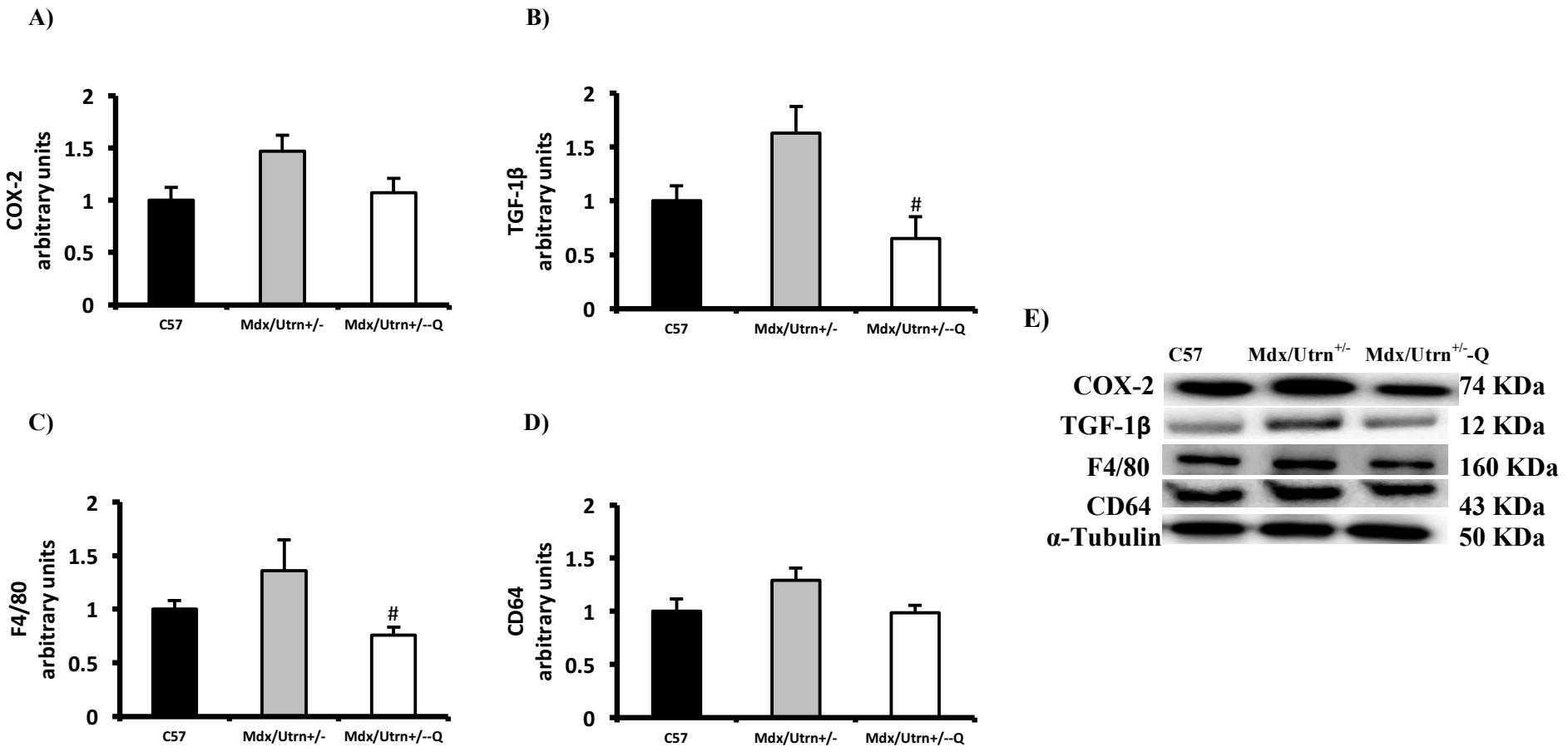
A)
COX-2 arbitrary units
2
1.5
1
0.5
0
C57
Mdx/Utrn+/-
Mdx/Utrn+/--Q
B)
TGF-1β arbitrary units
#
C)
F4/80 arbitrary units
D)
CD64 arbitrary units
E)
C57
Mdx/Utrn+/-
Mdx/Utrn+/--Q
COX-2
74 KDa
TGF-1β
12 KDa
F4/80
160 KDa
CD64
43 KDa
α-Tubulin
50 KDa

Figure 8

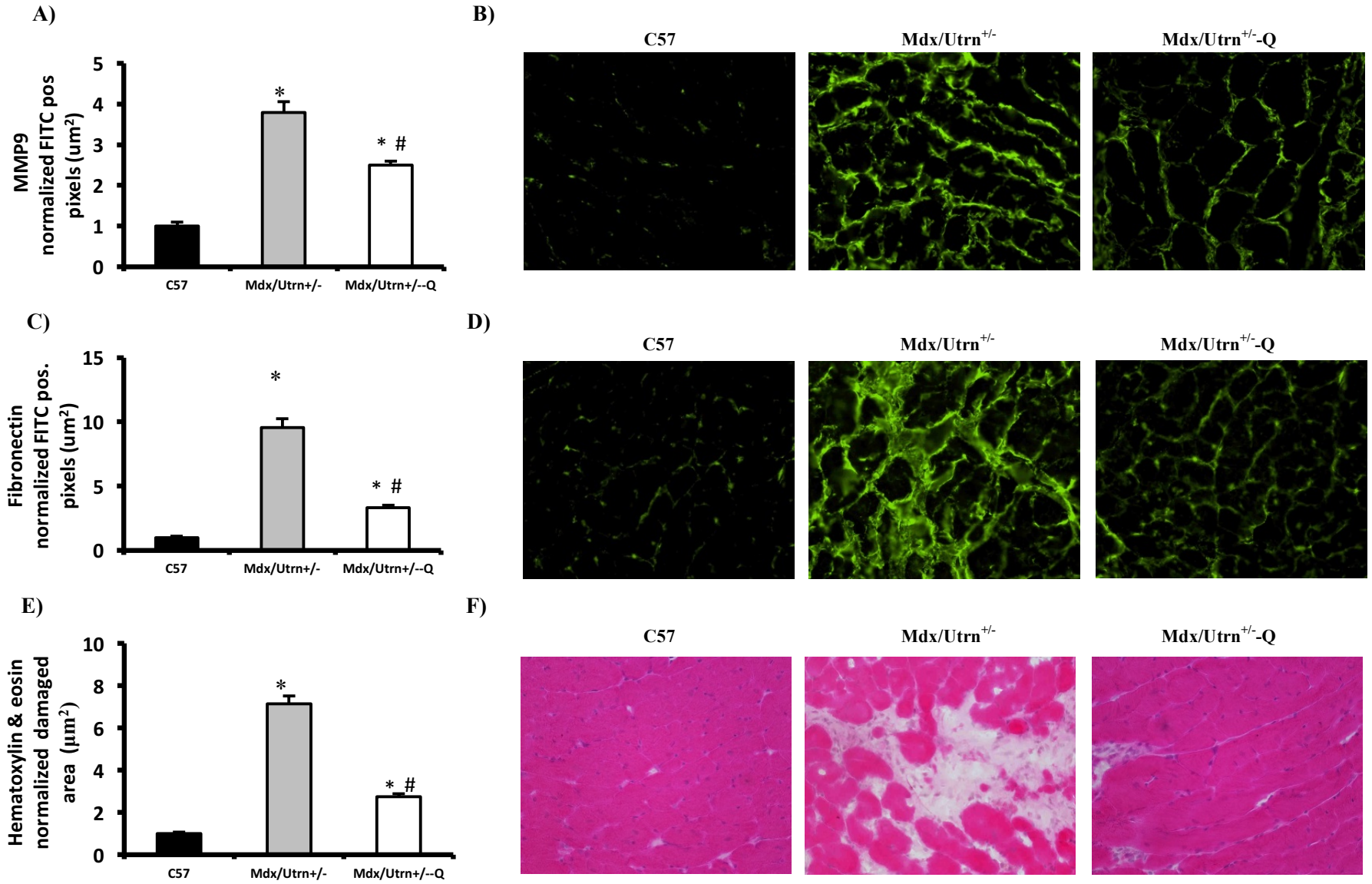
A)
B)
C)
D)
E)
F)
MMP9 normalized FITC pos pixels (um²)
Fibronectin normalized FITC pos. pixels (um²)
Hematoxylin & eosin normalized damaged area (µm²)
C57
Mdx/Utrn+/-
Mdx/Utrn+/--Q
Mdx/Utrn+/-
Mdx/Utrn+/-Q
0
1
2
3
4
5
0
5
10
15
0
2
4
6
8
10
*
* #

**Figure 9**

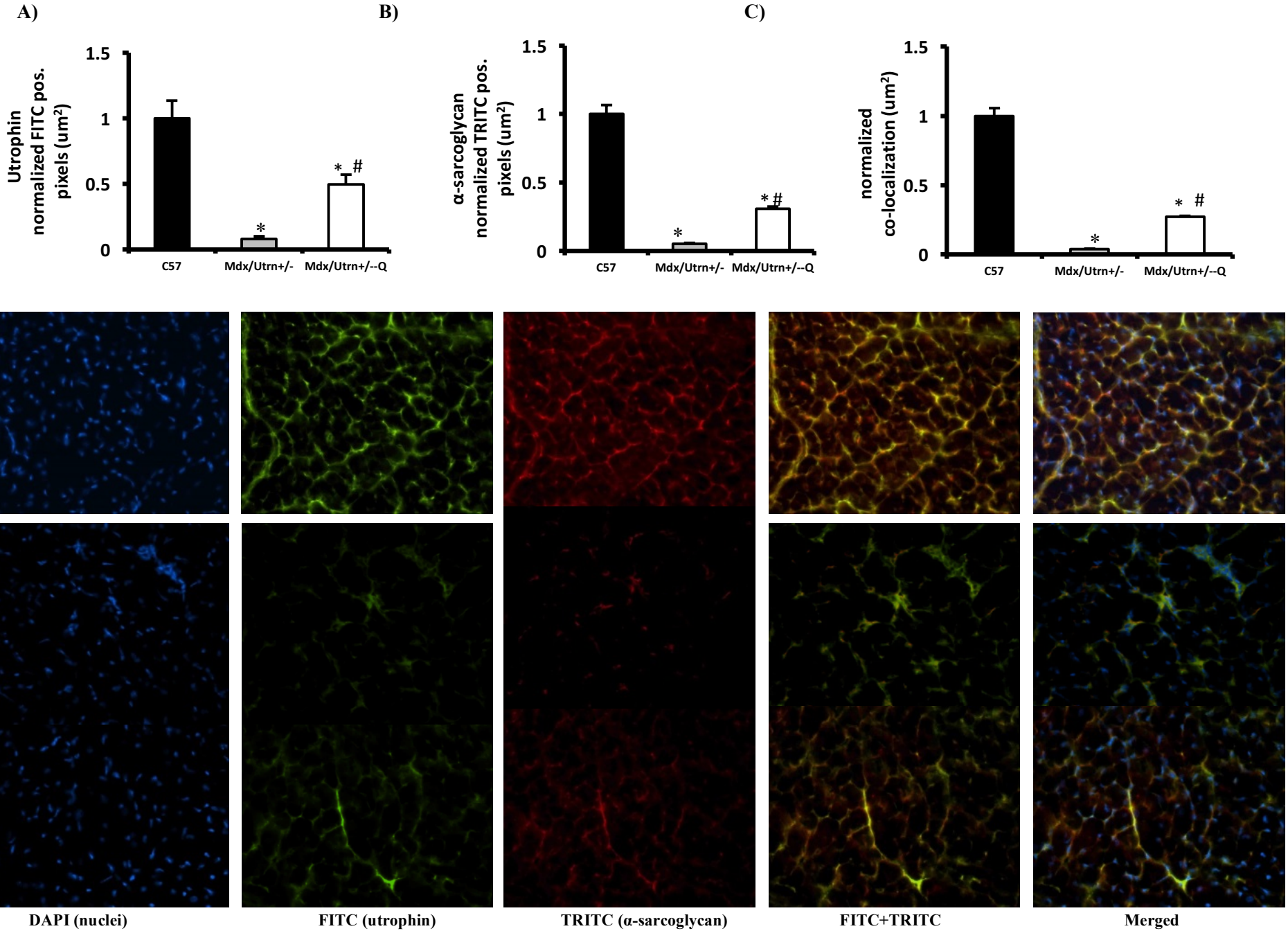
A)
B)
C)
Utrophin normalized FITC pos. pixels (um²)
α-sarcoglycan normalized TRITC pos. pixels (um²)
normalized co-localization (um²)
1.5
1
0.5
0
*
*#
C57
Mdx/Utrn+/-
Mdx/Utrn+/--Q
D)
C57
Mdx/ Utrn+/-
Mdx/ Utrn+/--Q
DAPI (nuclei)
FITC (utrophin)
TRITC (α-sarcoglycan)
FITC+TRITC
Merged

**Figure 10**